# CREEP-FATIGUE BEHAVIOR OF NiCoCrAlY COATED PWA 1480 SUPERALLOY SINGLE CRYSTALS

R.V. Miner, J. Gayda, and M.G. Hebsur
NASA Lewis Research Center
Cleveland, Ohio

The present study of high-temperature fatigue and creep-fatigue behavior is part of a program to identify the basic features of the effects of temperature, creep, fatigue, and environment on the behavior of a single-crystal superalloy, a bulk coating alloy, and a coated alloy system. A system was selected which has had considerable production experience: the Ni-base superalloy, PWA 1480, and the NiCoCrAlY coating, PWA 276, inventions of the Pratt & Whitney Aircraft Company.

Isothermal behavior was studied first. A series of fatigue and creep-fatigue tests of the types commonly designated as pp, cp, pc, and cc were conducted. These tests were conducted at various constant total strain ranges. The creep-fatigue cycles employed constant stress dwells at the maximum and/or minimum load. A complete set of data is published in a NASA Technical Memorandum (ref. 1).

## MATERIALS AND PROCEDURES

### Materials

PWA 1480, which is described in the literature (refs. 2 and 3), has the following nominal composition: 10 Cr, 5 Al, 1.5 Ti, 12 Ta, 4 W, 5 Co, and the balance Ni (in weight percent). The single crystals were solution treated for 4 hr at 1290 °C before machining. Bars having their <001> planes within less than 7° of the axis were selected. After machining, the LCF specimens were coated with PWA 276 by low-pressure plasma spraying. The coating composition (in weight percent) was 20 Co, 17 Cr, 12.4 Al, 0.5 Y, and the balance Ni. The coating thickness was about 0.12 mm. After coating, the specimens were given a diffusion treatment of 1080 °C for 4 hr and then aged at 870 °C for 32 hr.

## Test Procedures

The testing facility used in this investigation has been described in reference 4. Fatigue tests at 0.1 Hz and creep-fatigue tests were conducted using an hourglass type specimen and diametral strain control. The extensometer was always placed across one of the $\langle 001 \rangle$ planes nearly perpendicular to the specimen axis. Heating was produced by the passage of alternating current directly through the specimen.

After the first series of tests it was discovered that they had been conducted at 1015 °C, rather than at 1050 °C as intended. Also, it appeared that the dwell stress level affected life in the creep-fatigue cycles, but the result was somewhat confounded since the controlled dwell stresses and total strain ranges had been varied commensurately in order to minimize test times. In a second series of tests conducted at 1050 °C, total strain range and dwell stress level were varied as independently as practicable. However, life behavior in the lower temperature tests shows the same dependencies on strain and stress as in the 1050 °C tests, even though the two "independent" variables are more highly correlated.

All tests were controlled at constant total diametral strain range. However, the strains reported herein are calculated axial strains. In the creep-fatigue cycles constant stress dwells were employed. The first tests, those at 1015 °C, were controlled using an electromechanical programmer; in the 1050 °C tests a Data General S/20 computer was used. The frequency of the pp tests at both temperatures was about 0.1 Hz. The creep-fatigue tests employed about the same ramp rates as the pp tests.

# RESULTS

Some results of the 1050 and 1015 °C fatigue and creep-fatigue tests are shown in table I. Shown are the cycle type; cyclic life $N_f$; the values at half life of the total axial strain range $\Delta\epsilon_{tot}$, inelastic axial strain range $\Delta\epsilon_{in}$, stress range $\Delta\sigma$, and maximum stress $\sigma_{max}$; and the average cycle time $t_{av}$. Other data discussed below, such as that for the first cycle, may be found in reference 1.

## Constitutive Behavior

The constitutive behavior of PWA 1480 at 1015 and 1050 °C for all the stress dwell creep-fatigue cycle types studied is characterized by extreme cyclic softening. Inelastic axial strain range increased with cycling for all cycle types. At $0.5N_f$, $\Delta\epsilon_{in}$ had increased an average of ~25 percent for the pp tests,

~15 percent for the cp and pc tests, but generally less than 5 percent for the cc tests. For the 1050 °C tests the decrease in $\Delta\sigma$ at $0.5N_f$ averaged ~10 percent for the pp and cp tests but was slightly higher for the pc tests, ~15 percent. For the cp and pc tests at 1015 °C the decrease in $\Delta\sigma$ appeared to be smaller than for those tests at 1050 °C.

The most dramatic change with cycling in the creep-fatigue tests was the increase in creep rates. By $0.5N_f$, the reduction in cycle time was typically ~80 percent in the cp and pc tests and more than 95 percent in the cc tests, though the creep strain per cycle typically did not decrease during cycling. Creep strain did decrease as a fraction of the total inelastic strain range, however, and the fraction of pp strain increased. This occurred most in the 1050 °C tests.

Another interesting observation was that for the same absolute stress level, creep rates were higher in compression than in tension. This effect was observed in comparison of cp and pc tests but was most readily seen in the cc tests. Creep rates in compression were about 1.5 to 2 times higher than those in tension.

## Life Behavior

For both the fatigue and stress dwell creep-fatigue tests conducted in this study, the life of PWA 1480 correlated well with a model including both $\Delta\epsilon_{in}$ and $\Delta\sigma$. This model provides considerably better correlations than those based on $\Delta\epsilon_{in}$ alone, $\Delta\epsilon_{in}$ and $\sigma_{max}$, or $\Delta\epsilon_{in}$ and $t_{av}$.

Table II is a summary of the regression analyses for all test types at either test temperature using various power law models. These various models test the basic dependencies of life on frequency, strain rate, or $\sigma_{max}$ used in the strain-range-partitioning (ref. 5), frequency-separation (ref. 6), frequency-modified (ref. 7), and damage-rate (ref. 8) approaches.

The 1050 °C results will be examined first since they are clearer. As previously indicated, care was taken in the design of this series of tests to reduce as much as possible the correlation between the two "independent" variables in the creep-fatigue tests, total strain range, and dwell stress. The tests employed various total strain ranges but only two dwell stress levels in tension and/or compression. For this data set, even with the pp tests included, $\Delta\sigma$ and $\sigma_{max}$ are only 25 and 16 percent (R-values) correlated with $\Delta\epsilon_{in}$, respectively.

It may be seen in table II that the model $N_f = \alpha\ \Delta\sigma^{\gamma}$ provides a better fit than the single variable models containing $\Delta\epsilon$, $\sigma_{max}$, $t_{av}$, or any of the two-variable models not including $\Delta\sigma$. Neither the addition of $\sigma_{max}$ or $t_{av}$ to $\Delta\epsilon_{in}$ in the model provides substantial improvement. The model $N_f = \alpha\ \Delta\epsilon_{in}^{\beta}\ \Delta\sigma^{\gamma}$ provides the best fit of all. Note also that in the models containing $\sigma_{max}$ or $t_{av}$ together with $\Delta\epsilon$, the absolute values of the T-ratios for their coefficients are much less than 3, the usually accepted value for statistical significance. Plots of $N_{f,obs}$ and $N_{f,pred}$ are shown in figure 1 for the two models $N_f = \alpha\ \Delta\epsilon_{in}^{\beta}$ and $N_f = \alpha\ \Delta\epsilon_{in}^{\beta}\ \Delta\sigma^{\gamma}$.

Also, the model $N_f = \alpha\ \Delta\epsilon_{in}^{\beta}\ \Delta\sigma^{\gamma}$ provides the best fit for individual analyses of each cycle type. The best fit coefficients $\beta$ and $\gamma$ are not the same for each cycle type, as might be expected. Still, equations using the average values of $\beta$ and $\gamma$, -1.26 and -3.08, provide good fits for the individual cycle types. The values of $\alpha$ in these equations are shown in table III.

It is well demonstrated by the cc tests that $\Delta\sigma$ is more significant than $\sigma_{max}$ in determining life. Three tests were conducted with $\sigma_{max}$ and $\sigma_{min}$ of about +200/-200 MPa, or a $\Delta\sigma$ of about 400 MPa. An additional 1050 °C cc test, the first listed in table III, had about the same $\sigma_{max}$ (210 MPa) but a larger $\Delta\sigma$ (474 MPa). The life of this test was reduced to about 1/3 of that expected for a +200/-200 MPa test with the same $\Delta\epsilon_{in}$. In the fourth test listed in table II it was intended to increase $\sigma_{max}$ but keep $\Delta\sigma$ the same as for the first tests. Actually, $\sigma_{max}$ was increased about 30 percent to 257 MPa, but $\Delta\sigma$ was also increased about 10 percent, and still life increased relative to the +200/-200 MPa tests. For these cc tests alone, $R^2$ for the model $N_f = \alpha\ \Delta\epsilon_{in}^{\beta}\ \sigma_{max}^{\gamma}$ is 40 percent, only slightly better than the value of 37 percent for $N_f = \alpha\ \Delta\epsilon_{in}^{\beta}$, and considerably less than the value of 76 percent for $N_f = \alpha\ \Delta\epsilon_{in}^{\beta}\ \Delta\sigma^{\gamma}$.

For the tests at 1015 °C the model containing $\Delta\sigma$ alone provides no better correlation than that containing $\Delta\epsilon_{in}$; however, this could be explained by the high degree of correlation between $\Delta\sigma$ and $\Delta\epsilon_{in}$ in these tests, $R^2$ of 80 percent. Since $\Delta\epsilon_{in}$ is strongly correlated with $\Delta\sigma$, life correlates equally well with either variable. However, as for the tests at 1050 °C, $\sigma_{max}$ does not provide a good correlation, nor does $t_{av}$, and the model $N_f = \alpha\ \Delta\epsilon_{in}^{\beta}\ \Delta\sigma$ provides the best correlation. Figure 2 shows a comparison of the predictions of the models $N_f = \alpha\ \Delta\epsilon^{\beta}$

and $N_f = \alpha\ \Delta\epsilon^{\beta}\ \Delta\sigma^{\gamma}$. The best fit values of $\beta$ and $\gamma$ for the latter model are -1.00 and -2.70. Values of $\sigma$ which provide the best fit for each cyle type are shown in table III.

It may be seen that correlations using all the models are better for the 1015 °C data than for the 1050 °C data. This is largely because the 1015 °C data cover a greater range of the "independent" variables.

## Failure Mode

Internal crack initiation at pores was the predominant failure mode in these tests. For the creep-fatigue tests cracking initiated at many internal pores and linked up before the final overload in 80 percent of the specimens. Others appeared to have a dominant crack which initiated near the surface, possibly at a pore, but generally the fracture faces were heavily oxidized and difficult to interpret. Fracture surfaces with this appearance were more common for the pp tests. Still, the majority of pp tests failed at multiple internal pores.

## DISCUSSION

Except in that it permits inelastic strain, creep does not have a great effect on the cycle life of the coated single-crystal superalloy, PWA 1480. On any basis of comparison, and particularly on the basis of $N_f = \alpha\ \Delta\epsilon^{\beta}\ \Delta\sigma^{\gamma}$ as in table III, lives for the creep-fatigue cycles are not greatly, if at all, worse than those for the pp tests. Though life may be lower for the cp cycle than for the others, it is only about 30 percent lower than the average for the other cycles. Lives for the other cycles may all be the same.

In fact, there appears to be no time-dependent process having a great effect on life. This is shown by the lack of any substantial improvement when $t_{av}$ is included in the life models. Neither creep nor the environmental degradation have affected the coated single-crystal superalloy. The mechanisms of creep degradation in polycrystalline alloys such as grain boundary cavitation or sliding obviously cannot occur, and the environment cannot affect the internal crack propagation mode of failure.

The successful life model containing $\Delta\epsilon_{in}$ and $\Delta\sigma$ is unusual and may be peculiar to the coated single-crystal superalloy system studied. Crack initiation in high temperature creep-fatigue, at least for polycrystalline materials, is usually

found to be determined by $\Delta\epsilon_{in}$ and some measure of time-dependent damage processes such as creep cavitation at grain boundaries or oxidation attack. The importance of $\Delta\sigma$ in the life model and the internal crack initiation observed and may reflect that crack propagation is a significant portion of life in these texts. Since the cracks are protected from the atmosphere, it might be expected that the crack growth rates are relatively low, and, while crack initiation is thought to be primarily driven by $\Delta\epsilon_{in}$, $\Delta\sigma$ can be tied to crack propagation rates.

## RESULTS AND CONCLUSIONS

Fatigue tests at 0.1 Hz and cp, pc, and cc type creep-fatigue tests have been conducted on NiCoCrAlY coated specimens of a single-crystal superalloy, PWA 1480, at 1050 and about 1015 °C. The following results and conclusions were obtained:

1. Considerable cyclic softening occurred for all test cycles, evidenced particularly by rapidly increasing creep rates in the creep-fatigue tests.

2. Lives for the pp, cp, pc, and cc cycles were not greatly different; however, those for the cp cycle did appear to be lowest at both test temperatures.

3. A life model, $N_f = \alpha\, \Delta\epsilon_{in}^{\beta}\, \Delta\sigma^{\gamma}$, was found to provide good correlation for all cycle types, better than models based on $\Delta\epsilon_{in}$ alone, or $\Delta\epsilon_{in}$ with either $\sigma_{max}$ or $t_{av}$.

4. For all test types failure occurred predominantly by multiple internal cracking originating at porosity.

5. The strong correlation of life with $\Delta\sigma$ may reflect a significant crack growth period in the life of the specimens.

6. The lack of improvement in the models when average cycle time was considered appears to reflect that neither is there a large effect of strain rate on the damage mechanisms in the single-crystal material nor any environmental effect due to the internal cracking mode of failure

## REFERENCES


1. Miner, R.V.; Gayda, J.; and Hebsur, M.G.: Evaluation of Development Membranes for the Mixed Reactant Iron-Chromium Redox System. NASA TM-87110, 1985.

2. Gell, M.; Duhl, D.N.; and Giamei, A.F.: The Development of Single-Crystal Superalloy Turbine Blades. Superalloys 1980, ASM, Metals Park, OH 1980, pp. 205-214.

3. Shah, D.M.; and Duhl, D.N.: The Effect of Orientation, Temperature and Gamma Prime Size on the Yield Strength of a Single Crystal Nickel Base Supperalloy. Superalloys 1984, AIME, Warrendale, PA, 1984, pp. 105-114.

4. Hirshberg, M.H.: A Low Cycle Fatigue Testing Facility. Manual on Low Cycle Fatigue Testing, ASTM-STP 465, ASTM, 1969, pp. 67-86.

5. Manson, S.S.; Halford, G.R.; and Hirshberg, M.H.: Creep-Fatigue Analysis by Strain-Range Partitioning. Design for Elevated Temperature Environment, S.Y. Zamrik, ed., ASME, New York, 1971, pp. 12-24.

6. Coffin, L.F., Jr.: The Concept of Frequency Separation in Life Prediction for Time-Dependent Fatigue. Symposium on Creep-Fatigue Interaction, MPC-3, ASME, New York, pp. 349-363.

7. Ostergren, W.J.: Correlation of Hold Time Effects in Elevated Temperature Low Cycle Fatigue Using a Frequency Modified Damage Function. Symposium on Creep-Fatigue Interaction, MPC-3, ASME, New York, pp. 179-202.

8. Majumdar, S.; and Maiya, P.S.: A Damge Equation for Creep-Fatigue Interaction. Symposium on Creep-Fatigue Interaction, MPC-3, ASME, New York, pp. 323-336.

TABLE I. - LOW-CYCLE FATIGUE DATA FOR COATED PWA 1480 SINGLE CRYSTALS

[Values of $\Delta\epsilon_{in}$, $\Delta\sigma$, and $\sigma_{max}$ are those at half life.]

| Cycle type | Cycle life, $N_f$ | Total axial strain range, $\Delta\epsilon_{tot}$, percent | Inelastic axial strain range, $\Delta\epsilon_{in}$, percent | Stress range, $\Delta\sigma$, MPa | Maximum stress, $\sigma_{max}$, MPa | Average, cycle time, $t_{av}$, min |
|---|---|---|---|---|---|---|
| Test temperature, 1050 °C | | | | | | |
| pp | 110 | 1.86 | 0.92 | 766 | 388 | 0.17 |
| | 580 | 1.29 | .47 | 631 | 331 | .17 |
| | 900 | 1.26 | .52 | 571 | 292 | .17 |
| | 950 | 1.05 | .32 | 552 | 272 | .17 |
| | 1000 | 1.16 | .47 | 537 | 274 | .17 |
| | 2900 | .87 | .30 | 416 | 210 | .17 |
| cp | 85 | 2.04 | 1.20 | 655 | 255 | 1.14 |
| | 160 | 1.50 | 0.82 | 528 | 197 | 1.28 |
| | 300 | 1.53 | .81 | 559 | 163 | .35 |
| | 440 | 1.30 | .69 | 465 | 206 | .31 |
| | 810 | 1.27 | .60 | 505 | 201 | .50 |
| | 1150 | 1.12 | 0.52 | 438 | 201 | .40 |
| pc | 195 | 1.62 | 0.85 | 625 | 376 | 0.60 |
| | 610 | 1.62 | .81 | 639 | 379 | .50 |
| | 930 | 1.42 | .76 | 592 | 287 | .63 |
| | 1250 | 1.58 | .91 | 490 | 266 | .60 |
| | 1410 | 1.54 | .90 | 445 | 225 | .40 |
| | 1650 | 1.30 | .71 | 419 | 225 | .40 |
| | 1700 | 1.12 | .52 | 445 | 247 | .24 |
| cc | 370 | 1.32 | 0.70 | 474 | 210 | 0.78 |
| | 790 | 1.41 | .87 | 412 | 206 | .64 |
| | 990 | 1.20 | .68 | 403 | 206 | .49 |
| | 1100 | 1.30 | .74 | 439 | 257 | 1.45 |
| | 2110 | .90 | .30 | 400 | 199 | .30 |
| Test temperature, 1015 °C | | | | | | |
| pp | 174 | 1.81 | 0.62 | 904 | 457 | 0.14 |
| | 192 | 2.02 | .81 | 941 | 478 | .16 |
| | 2021 | 1.08 | .38 | 521 | 275 | .15 |
| | 2314 | .85 | .15 | 529 | 276 | .15 |
| | 3900 | .77 | .16 | 438 | 227 | .12 |
| | 7870 | .05 | .05 | 344 | 166 | .15 |
| cp | 15 | 3.32 | 1.95 | 1090 | 429 | 15.3 |
| | 78 | 1.85 | 1.16 | 802 | 270 | 4.8 |
| | 146 | 1.18 | .40 | 680 | 206 | 4.6 |
| | 218 | 1.51 | .58 | 644 | 208 | 2.4 |
| | 610 | .90 | .30 | 531 | 345 | 15.0 |
| pc | 29 | 2.44 | 1.37 | 826 | 569 | 22.1 |
| | 54 | 2.01 | .88 | 856 | 394 | 14.7 |
| | 340 | 1.43 | .62 | 603 | 396 | 3.92 |
| | 730 | 1.10 | .34 | 613 | 395 | 1.23 |
| | 2101 | .50 | .30 | 468 | 276 | 1.26 |
| cc | 192 | 1.63 | 0.98 | 514 | 257 | 7.38 |
| | 724 | 1.37 | .72 | 499 | 250 | .45 |
| | 1826 | .88 | .30 | 436 | 218 | .59 |

TABLE II. - FIT OF VARIOUS MODELS RELATING LOG $N_f$ FOR ALL CYCLE TYPES TO THE LOG OF SEVERAL SINGLE VARIABLES OR COMBINATIONS THEREOF

| Temperature, °C | Variable | | | | | | | | | | s | $R^2$, percent |
|---|---|---|---|---|---|---|---|---|---|---|---|---|
| | Constant | | log $\Delta\varepsilon_{in}$ | | log $\Delta\sigma$ | | log $\sigma_{max}$ | | log $t_{av}$ | | | |
| | $\alpha$ | T | Coef-ficient | T | Coef-ficient | T | Coef-ficient | T | Coef-ficient | T | | |
| 1050 | -0.792 | -0.8 | -1.65 | -3.7 | | | | | | | 0.32 | 37 |
| | 12.772 | 6.1 | | | -3.683 | -4.8 | | | | | .29 | 50 |
| | 5.602 | 2.8 | | | | | -1.159 | -1.4 | | | .39 | 8 |
| | 3.037 | 22. | | | | | | | -0.466 | -1.7 | .38 | 12 |
| | 8.396 | 4.2 | -1.258 | -3.8 | -3.077 | -4.9 | | | | | .23 | 70 |
| | 1.218 | 0.6 | -1.578 | -3.5 | | | -0.765 | -1.1 | | | .32 | 40 |
| | -1.297 | -1.1 | -1.927 | -3.1 | | | | | 0.199 | 0.6 | .33 | 38 |
| 1015 | -1.505 | -3.1 | -1.762 | -8.5 | | | | | | | .34 | 81 |
| | 16.427 | 9.8 | | | -4.958 | -8.2 | | | | | .33 | 80 |
| | 10.287 | 4.5 | | | | | -3.091 | -3.4 | | | .60 | 40 |
| | 2.689 | 21.7 | | | | | | | -0.654 | -4.3 | .53 | 52 |
| | 7.781 | 3.0 | -1.003 | -3.8 | -2.696 | -3.6 | | | | | .26 | 90 |
| | 0.424 | 0.2 | -1.607 | -6.1 | | | -0.63 | -1.0 | | | .34 | 82 |
| | -0.706 | -1.4 | -1.433 | -6.2 | | | | | -0.251 | -2.3 | .30 | 86 |

TABLE III. - BEST FIT VALUES $\alpha$ IN THE LIFE MODELS FOR 1050 and 1015 °C

| Cycle type | $\alpha$ | 95 percent confidence limits on $\alpha \times 10^{-8}$ |
|---|---|---|
| 1050 °C: $N_f = \alpha \Delta\varepsilon_{in}^{-1.26} \Delta\sigma^{-3.08}$ | | |
| pp | $2.25 \times 10^8$ | 1.8 to 2.9 |
| cp | 1.41 | 1.0 to 2.0 |
| pc | 3.66 | 2.4 to 5.5 |
| cc | 1.86 | 1.2 to 2.9 |
| 1015 °C: $N_f = \alpha \Delta\varepsilon_{in}^{-1.00} \Delta\sigma^{-2.70}$ | | |
| pp | $0.489 \times 10^8$ | 0.24 to 0.98 |
| cp | .236 | .16 to 0.35 |
| pc | .318 | .17 to 0.60 |
| cc | .360 | .11 to 1.18 |

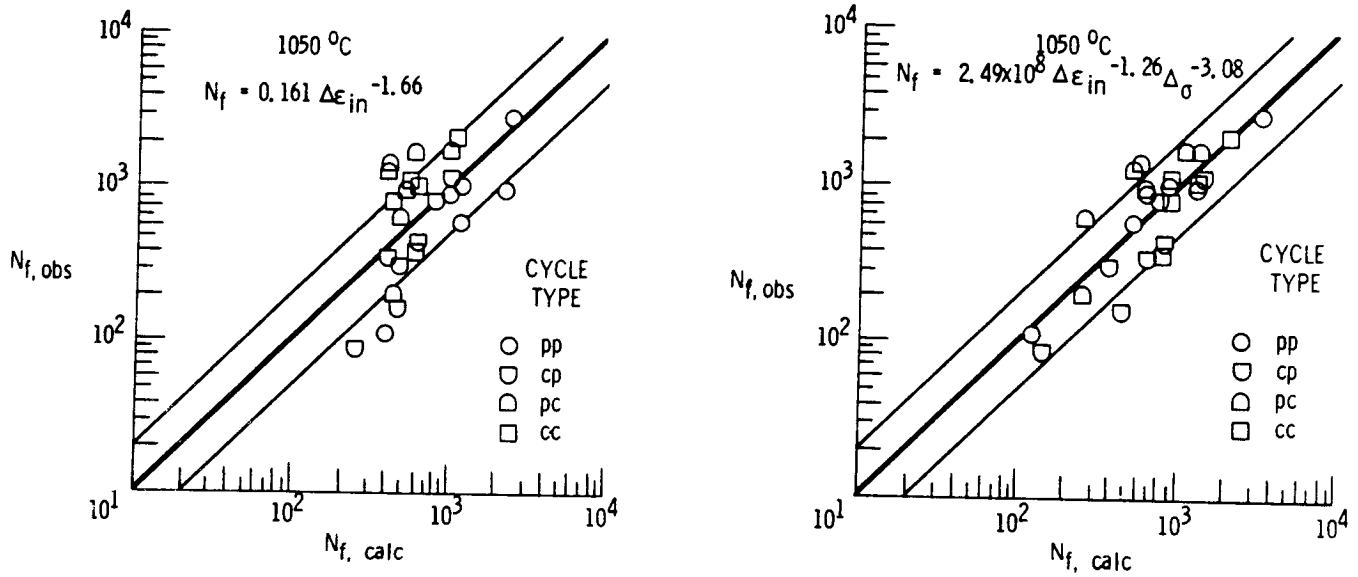


Figure 1. Observed vs. calculated cyclic life at 1050°C for life models indicated.

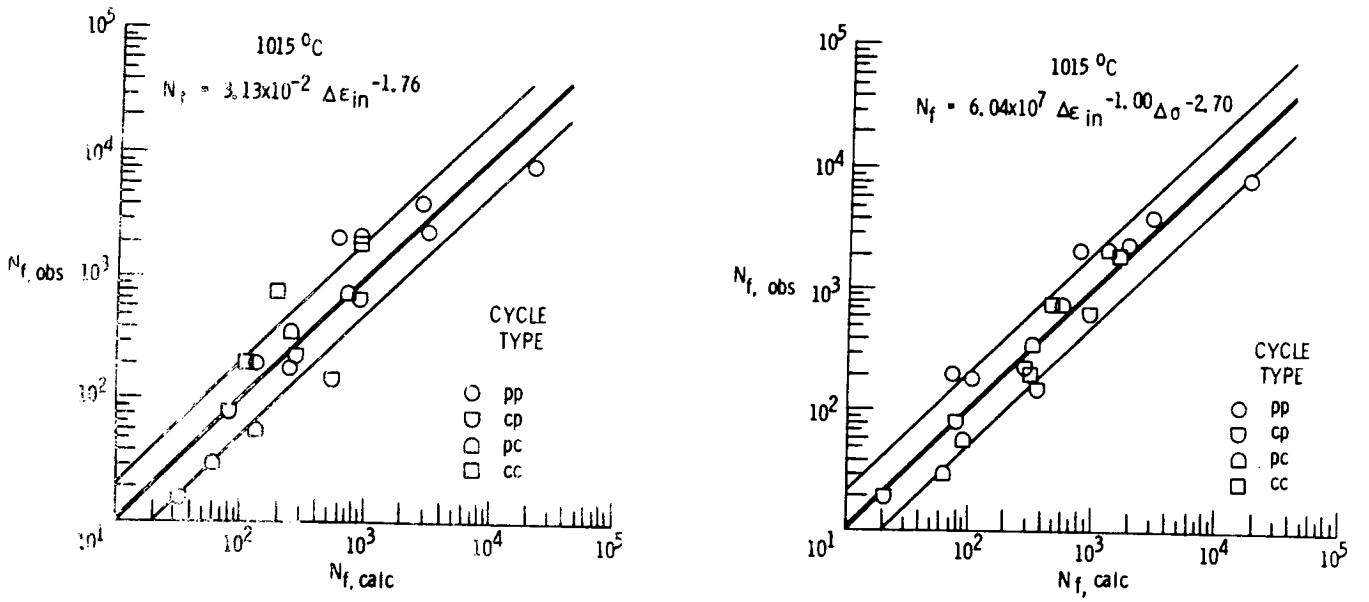


Figure 2. Observed vs. calculated cyclic life at 1015°C for life models indicated.